PAPER

Stability Analysis of XCP (eXplicit Control Protocol) with Heterogeneous Flows

Yusuke SAKUMOTO[†a], ***Student Member***, **Hiroyuki OHSAKI**[†b], ***and*** **Makoto IMASE**[†c], ***Members***

SUMMARY   In this paper, we analyze the stability of XCP (eXplicit Control Protocol) in a network with heterogeneous XCP flows (i.e., XCP flows with different propagation delays). Specifically, we model a network with heterogeneous XCP flows using fluid-flow approximation. We then derive the conditions that XCP control parameters should satisfy for stable XCP operation. Furthermore, through several numerical examples and simulation results, we quantitatively investigate effect of system parameters and XCP control parameters on stability of the XCP protocol. Our findings include: (1) when XCP flows are heterogeneous, XCP operates more stably than the case when XCP flows are homogeneous, (2) conversely, when variation in propagation delays of XCP flows is large, operation of XCP becomes unstable, and (3) the output link bandwidth of an XCP router is independent of stability of the XCP protocol.
key words: XCP (eXplicit control protocol), stability, heterogeneous flows, control theory, fluid-flow approximation

1. Introduction

TCP (Transmission Control Protocol) is being widely used in the Internet to carry data traffic [1]. There are various versions of TCP, and the most popular ones are TCP version Reno (TCP Reno) and its variants [2]. Several problems of TCP Reno have been reported such as its inability to support rapidly increasing speeds of recent networks [3]–[5].

One of the serious problems with TCP Reno is that a large number of packets sent into the network are discarded. This problem is caused by inability of source hosts to detect congestion before some packets are lost, and large delay for source hosts to detect congestion when the round-trip time between end hosts is large. Since the scale and the speed of network is continuously increasing, it is expected that the performance of TCP Reno would be further degraded due to an increased number of packet losses before source hosts' congestion detection.

For solving such problems in a high-speed and wide-area network, many transport-layer protocols using explicit feedback from a router to end hosts are proposed [6]–[9]. Compared with TCP Reno, these protocols perform efficient congestion control between end hosts with the aid of routers. Among those router-assisted congestion control mechanisms, XCP (eXplicit Control Protocol) has been receiving attention [6], [10]. XCP is a sort of window-based

flow control mechanisms. An XCP router periodically calculates the amount of window size increase/decrease for a source host, and notifies source hosts of it as explicit feedback. With such explicit feedback, an XCP source host can quickly and appropriately respond to congestion status of the network.

With simulation experiments, it has been reported that XCP achieves better performance than TCP Reno does [6], [11]. However, characteristics of XCP as a feedback-based control system, such as stability and transient performance, have not been sufficiently clarified.

A stability issue of XCP in a tandem network has been pointed out in [12] through simulation experiments. In [12], the authors show that the operation of XCP may become unstable in a tandem network. Due to the nature of the simulation-based and subjective approach taken in [12], detailed characteristics of XCP protocol has not been clarified. For better understanding the characteristics of the XCP protocol, analytic approaches are indispensable.

There exist a few analytical studies on XCP, all of which used fluid-flow approximation [6], [13]–[15]. In [6], [13], by assuming an identical propagation delay for all XCP flows, stability of XCP has been analyzed. The authors of [6] have derived a sufficient condition for XCP control parameters to stabilize XCP's operation. By extending the analytic model in [6], the authors of [13] have shown that operation of XCP becomes unstable when the available bandwidth of an XCP router's output link is varied. The authors of [14] have analyzed stability of XCP using a Lyapunov function. In [14], the authors mention possibility of extending their stability analysis to handle heterogeneous XCP flows, but the details are not presented. In [15], steady state performance of XCP in a tandem network (i.e., a network with multiple routers and heterogeneous flows) has been analyzed. Specifically, the authors of [15] have derived throughput of XCP flows in steady state, and have shown that fairness among XCP flows is significantly degraded unless control parameters of an XCP router are configured appropriately. Although multiple XCP flows are modeled in [15] for analyzing fairness among XCP flows, stability of XCP has not been investigated.

In this paper, we analyze the stability of XCP in a network with heterogeneous XCP flows (i.e., XCP flows with different propagation delays). Specifically, we model a network with heterogeneous XCP flows using fluid-flow approximation. We then derive the conditions that XCP control parameters should satisfy for stable XCP operation.

Through several numerical examples and simulation results, we quantitatively investigate effect of system parameters and XCP control parameters on stability of the XCP protocol. Our findings include: (1) when XCP flows are heterogeneous, XCP operates more stably than the case when XCP flows are homogeneous, (2) conversely, when variation in propagation delays of XCP flows are large, operation of XCP becomes unstable, and (3) the output link bandwidth of an XCP router is independent of stability of the XCP protocol.

The primary contribution of this paper is to mathematically reveal stability properties of the XCP protocol with heterogeneous flows. Different from [12], [15], we explicitly model the dynamics of heterogeneous XCP flows for deriving the stability condition. Our stability analysis is based on [16], which analyzes the stability of the DCCP protocol. We believe our findings are *generic* since our stability analysis is performed with reasonable assumptions (see Sect. 3), as well as *valid* since our stability analysis is validated through simulations in Sect. 5.

The organization of this paper is as follows. First, in Sect. 2, the algorithm of XCP is briefly explained. In Sect. 3, heterogeneous XCP flows and an XCP router are modeled using fluid-flow approximation. Section 4 performs stability analysis of XCP. In Sect. 5, the effect of system parameters and XCP control parameters on stability of the XCP protocol is quantitatively evaluated through several numerical examples and simulation results. Finally, in Sect. 6, we conclude this paper and discuss future works.

2. XCP (eXplicit Control Protocol)

In this section, the congestion control algorithm of XCP is briefly summarized. Refer to [6] for details of the XCP algorithm.

In XCP, congestion information is exchanged between a source host and a router using *congestion header* in a packet. An overview of the XCP congestion control using the congestion header of a packet is illustrated in Fig. 1.
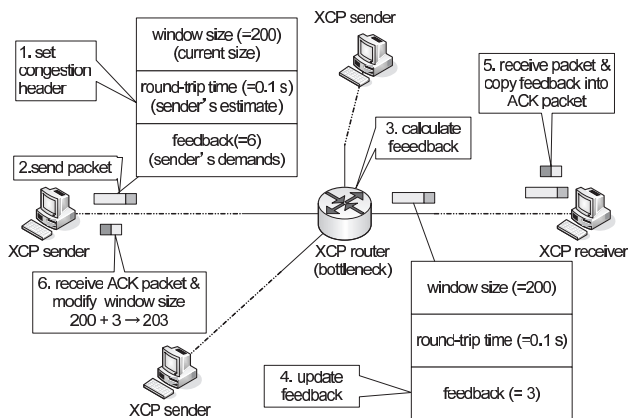

Fig. 1 Overview of XCP congestion control algorithm; a router calculates the amount of window size increase/decrease for a source host, and it then notifies the source host of the calculated value as explicit feedback.

XCP is a sort of window-based flow control mechanisms. In XCP, a router calculates the amount of window size increase/decrease for a source host, and it then notifies the source host of the calculated value as explicit feedback. The congestion header of a packet stores information on a source host and a router: e.g., the window size and the estimated round-trip time of the source host, and the amount of window-size increase/decrease (i.e., feedback value) calculated by the router.

At the time of packet transmission, a source host stores its estimated round-trip time, its current window size, and the initial value of the feedback value (i.e., the amount of window size increase requested by the source host) in the congestion header of the packet. This enables the XCP router to know the status of the source host.

When the packet arrives at an XCP router, the router calculates a feedback value based on the information stored in the congestion header of the packet. The router overwrites the feedback value in the congestion header of the packet with the calculated feedback value, if the feedback value stored in the congestion header is larger than the calculated feedback value. The XCP router then forwards the packet to its downstream router.

Once the packet arrives at a destination host, the destination host returns an ACK (ACKnowledgement) packet to the source host. At this time, the congestion header of the data packet is copied to the congestion header of the ACK packet. This makes it possible for the source host to know the congestion information of XCP routers by way of the destination host.

Finally, when the source host receives the ACK packet, the feedback value stored in the congestion header of the ACK packet is added to the current window size of the source host.

In what follows, we explain how an XCP router calculates a feedback value (i.e., the amount of increase/decrease of the window size of a source host).

The control mechanism of an XCP router is composed of *efficiency controller*, which tries to maximize utilization of the router, and *fairness controller*, which tries to realize fairness among competing XCP flows. The efficiency controller and the fairness controller are invoked every average round-trip time of all XCP flows. The efficiency controller calculates the total amount of rate increase/decrease for all XCP flows. The fairness controller then calculates the amount of rate increase/decrease for each XCP flow. An XCP router calculates a feedback value based on the amount of rate increase/decrease calculated by the fairness controller and information stored in the congestion header of arriving packets. In what follows, algorithms of the efficiency controller and the fairness controller are briefly explained.

The efficiency controller calculates the aggregate feedback value ϕ (i.e., the total amount of rate increase/decrease for all XCP flows) from the packet arrival rate at the XCP router and the current queue length as

$$\phi = \alpha\, d\, S - \beta\, Q, \tag{1}$$

where d is the average round-trip time of XCP flows accommodated in the XCP router, S is the available bandwidth of the link (i.e., the output link bandwidth excluding the current packet arrival rate), Q is the minimum queue length observed during the average round-trip propagation time, and α and β are control parameters of the XCP router.

The fairness controller distributes the aggregate feedback value ϕ to all XCP flows. The fairness controller realizes fairness among XCP flows by performing an AIMD (Additive Increase and Multiplicative Decrease) control. Namely, if $\phi \geq 0$, the fairness controller allocates ϕ so that the increase in throughput of all XCP flows is the same. On the contrary, if $\phi < 0$, the fairness controller allocates ϕ so that the decrease in throughput of a XCP flow is proportional to its current throughput. Specifically, the fairness controller calculates ξ_p and ξ_n, which are used for calculating the feedback value.

$$\xi_p = \frac{h + [\phi]^+}{d \sum_{m=1}^{N} \frac{rtt_m\, s_m}{w_m}} \tag{2}$$

$$\xi_n = \frac{h + [-\phi]^+}{d\, T} \tag{3}$$

In the above equations, N is the number of packets arrived at the XCP router during the average round-trip time, and T is the total size of packets arrived during the average round-trip time.

Also, w_m and rtt_m are the window size and the estimated round-trip time stored in the congestion header of the m-th packet of N packets arrived during the average round-trip time, and s_m is the packet size of the m-th packet. Note that $[x]^+ \equiv \max(x, 0)$.

In Eq. (3), h is called *shuffle traffic*, and is determined by

$$h = [\gamma T - |\phi|]^+, \tag{4}$$

where γ is a control parameter of an XCP router.

Finally, an XCP router calculates the feedback value $H_{feedback}$ for the m-th packet as

$$H_{feedback} = \xi_p\, \frac{rtt_m^2\, s_m}{w_m} - \xi_n\, rtt_m\, s_m. \tag{5}$$

3. Modeling with Fluid-Flow Approximation

In this paper, we model a network with heterogeneous XCP flows with different propagation delays (i.e., XCP flows traversing links with different propagation delays) sharing the single bottleneck link as a discrete-time system (Fig. 2). XCP flows are classified into *flow classes*, in which XCP flows have the identical propagation delay. In our analysis, dynamics of transfer rates from XCP flows and the queue length of an XCP router are modeled as discrete-time models with slot length of Δ. The definition of symbols used throughout our analysis is summarized in Table 1.
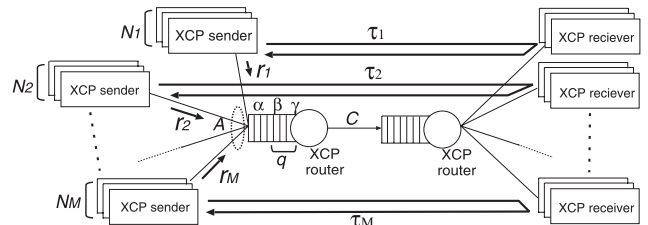

Fig. 2 Analytic model; heterogeneous XCP flows with different propagation delays share the single bottleneck.

Table 1 The definition of symbols.

M	the number of flow classes
N_i	the number of XCP flows in flow class i
Δ	slot length
r_i	transfer rate of XCP flows in flow class i
τ_i	two-way propagation delay of XCP flows in flow class i
d	average round-trip time of all XCP flows
s	packet length
T	the total size of packets arrived during the average round-trip time
q	current queue length of XCP router
ϕ	aggregate feedback of XCP router
h	shuffle traffic of XCP router
A	packet arrival rate at XCP router
C	output link bandwidth of XCP router
α	XCP control parameter
β	XCP control parameter
γ	XCP control parameter

In this paper, we focus on the stability of XCP in a network with a single XCP router, rather than in a tandem network. We believe that it is possible to extend our analytic approach to a tandem network with multiple XCP routers, but it is beyond the scope of this paper. It should be noted that the operation of XCP may become unstable in a tandem network when many XCP flows are frequently activated and/or deactivated [12]. The main purpose of this paper is, however, to investigate the effect of heterogeneous flow on the stability of the XCP protocol.

In what follows, using a fluid-based modeling approach, we derive a detailed model of a network with heterogeneous XCP flows.

First, we model dynamics of the transfer rate of an XCP flow. In our analysis, we assume: (a) all XCP flows with the same propagation delay synchronize, (b) all XCP source hosts always have data to transfer, (c) sizes of all packets are equal, (d) the window size of a source host is changed only by receiving the feedback value from XCP routers (i.e., effect of timeouts triggered by a large number of packet losses are negligible), and (e) the round-trip time of an XCP flow is equal to its two-way propagation delay.

Since an XCP router performs the same congestion control for all XCP flows with the same round-trip time (see Eq. (5)), the assumption (a) is reasonable. Moreover, since XCP is mainly used for transferring a large amount of data in a high-speed network, assumptions (b) through (d) should be appropriate. The assumption (e) is reasonable since the control objective of an XCP router is to minimize

its queue length, resulting negligible queuing delay at the router buffer. Note that in our analysis, all XCP flows are assumed to start their transmissions simultaneously from an initial state. Hence, the queue length of the XCP router is not likely to be overloaded, which validates the assumption (e).

The transfer rate and the two-way propagation delay of XCP flows in flow class i are denoted by r_i and τ_i, respectively. Moreover, the number of XCP flows in flow class i is denoted by N_i. Then, the packet arrival rate A at an XCP router and the average round-trip time d of all XCP flows are given by

$$A = \sum_{i=1}^{M} N_i\, r_i, \tag{6}$$

$$d = \frac{\sum_{i=1}^{M} N_i\, \tau_i}{\sum_{i=1}^{M} N_i}. \tag{7}$$

Since $\sum_{m=1}^{N} rtt_m\, s_m/w_m \simeq d \sum_{i=1}^{M} N_i$ in Eq. (2) [15] and $T \simeq A\, d$, ξ_p and ξ_n (Eqs. (2) and (3)) are given by

$$\xi_p = \frac{h + [\phi]^+}{d^2 \sum_{i=1}^{M} N_i}, \tag{8}$$

$$\xi_n = \frac{h + [-\phi]^+}{d^2 A}. \tag{9}$$

In the above equations, the aggregate feedback value ϕ and the shuffle traffic h are given by Eqs. (1) and (4) as

$$h = [\gamma\, d\, A - |\phi|]^+, \tag{10}$$
$$\phi = \alpha\, d\, (C - A) - \beta\, q, \tag{11}$$

where q is the current queue length of the XCP router, and C is the output link bandwidth of the XCP router.

From Eqs. (8) and (9), the feedback value $H_{feedback_i}$ for XCP flows in flow class i is given by

$$H_{feedback_i} = \frac{h + [\phi]^+}{d^2 \sum_{j=1}^{M} N_j} \frac{\tau_i\, s}{r_i} - \frac{h + [-\phi]^+}{d^2 A} \tau_i\, s. \tag{12}$$

Hence, at the time of ACK packet reception, the amount of change in the transfer rate of XCP flows in flow class i is given by

$$\frac{H_{feedback_i}}{\tau_i} = \frac{h + [\phi]^+}{d^2 \sum_{j=1}^{M} N_j} \frac{s}{r_i} - \frac{h + [-\phi]^+}{d^2 A} s. \tag{13}$$

The transfer rate of XCP flows in flow class i and the current queue length of the XCP router at slot k are denoted by $r_i(k)$ and $q(k)$, respectively. Without loss of generality, we assume that the propagation delay from a source host to the XCP router is zero, and that the propagation delay from the XCP router to source hosts by way of the destination hosts is τ_i. The information stored in the congestion header of the ACK packet received by a source host at slot k is $k - \tau_i/\Delta$ slots old. Moreover, the number of ACK packets that a source host receives during the slot length Δ can be approximated by $r_i(k - \tau_i/\Delta)\, \Delta/s$. Thus, from Eq. (13), the

transfer rate of XCP flows in flow class i at $(k + 1)$-th slot is given by

$$r_i(k + 1) \simeq r_i(k) + \Delta \frac{h(k - \frac{\tau_i}{\Delta}) + [\phi(k - \frac{\tau_i}{\Delta})]^+}{d^2 \sum_{j=1}^{M} N_j}$$
$$- \Delta \frac{r_i(k - \frac{\tau_i}{\Delta})\left(h(k - \frac{\tau_i}{\Delta}) + [-\phi(k - \frac{\tau_i}{\Delta})]^+\right)}{d^2 A(k - \frac{\tau_i}{\Delta})}. \tag{14}$$

Next, we model the dynamics of the queue length of an XCP router. Letting $q(k)$ be the current queue length of the XCP router at slot k, the current queue length $q(k + 1)$ at slot $k + 1$ is approximately given by

$$q(k + 1) \simeq \begin{cases} q(k) + \Delta\, (A(k) - C) & \text{if } q(k) > 0 \\ q(k) + \Delta\, [A(k) - C]^+ & \text{if } q(k) = 0 \end{cases}. \tag{15}$$

4. Stability Analysis

In what follows, using the fluid-flow model of XCP derived in Sect. 3, we analyze the stability (local asymptotic stability) of XCP around its equilibrium point using the same analytic approach with [16]. In what follows, equilibrium values of the transfer rate $r_i(k)$ and the current queue length $q(k)$ are denoted by r_i^* and q^*, respectively. First, we linearize the fluid-flow model defined by Eqs. (14) and (15) at its equilibrium point. The aggregate feedback value $\phi(k)$ and the current queue length $q(k)$ are discontinuous at the equilibrium point (i.e., $\phi^* = 0$ and $q^* = 0$). For alleviating such a discontinuity problem, we introduce the following approximation for a sufficiently small Δ.

$$\frac{[f(x + \Delta)]^+ - [f(x)]^+}{\Delta} \simeq \frac{1}{2} \frac{f(x + \Delta) - f(x)}{\Delta} \tag{16}$$

Thereby, Eqs. (14) and (15) can be approximated as

$$r_i(k + 1) \simeq r_i(k) + \Delta \frac{h(k - \frac{\tau_i}{\Delta}) + \phi(k - \frac{\tau_i}{\Delta})/2}{d^2 \sum_{j=1}^{M} N_j}$$
$$- \Delta \frac{r_i(k - \frac{\tau_i}{\Delta})\left(h(k - \frac{\tau_i}{\Delta}) - \phi(k - \frac{\tau_i}{\Delta})/2\right)}{d^2 A(k - \frac{\tau_i}{\Delta})}, \tag{17}$$

and

$$q(k + 1) \simeq q(k) + \frac{\Delta\, (A(k) - C)}{2}. \tag{18}$$

Equations (17) and (18) suggest that state variables at slot $k + 1$ are determined by state variables from $k - \nu$ ($\nu \equiv \max_{1 \le i \le M} \tau_i/\Delta$) to slot k.

Furthermore, we linearize Eq. (17) around its equilibrium point as

$$r_i(k + 1) \simeq \sum_{m=1}^{M} \sum_{n=0}^{\nu} \frac{\partial r_i(k + 1)}{\partial r_m(k - n)} \{r_m(k - n) - r_m^*\}$$
$$+ \sum_{n=0}^{\nu} \frac{\partial r_i(k + 1)}{\partial q(k - n)} \{q(k - n) - q^*\}. \tag{19}$$

We introduce a state vector $\mathbf{x}(k)$ that is composed of differences between each state variable at slot $k, \ldots, k - \nu$ and their equilibrium values.

$$\mathbf{x}(k) = \begin{pmatrix} r_1(k) & - & r_1^* \\ & \vdots & \\ r_1(k - \nu) & - & r_1^* \\ & \vdots & \\ r_M(k) & - & r_M^* \\ & \vdots & \\ r_M(k - \nu) & - & r_M^* \\ q(k) & - & q^* \\ & \vdots & \\ q(k - \nu) & - & q^* \end{pmatrix} \quad (20)$$

The relation between $\mathbf{x}(k)$ and $\mathbf{x}(k + 1)$ can be represented using a state transition matrix $\mathbf{B}$ as

$$\mathbf{x}(k + 1) = \mathbf{B}\,\mathbf{x}(k). \quad (21)$$

Note that the state transition matrix $\mathbf{B}$ is independent of the slot k. If $\mathbf{x}(k)$ converges to the zero vector for $k \to \infty$, the system is stable. Otherwise, the system is unstable. The state transition matrix $\mathbf{B}$ determines the stability of the system. Let $\lambda_i (1 \le i \le (M + 1)(\nu + 1))$ be the eigenvalues of the state transition matrix $\mathbf{B}$. The maximum absolute value of eigenvalues (i.e., maximum modules) determines the stability around its equilibrium point. It is known that the system is stable if the maximum modulus is less than unity [17]. Namely, if the maximum modulus is less than unity, $x(k)$ converges to the zero vector for $k \to \infty$.

5. Numerical Examples and Simulation Results

5.1 Experimental Design

In this section, through several numerical examples and simulation results, we investigate the effect of system parameters and XCP control parameters on stability of XCP protocol. Due to space limitation, in what follows, only results in the case of two flow classes ($M = 2$) are shown. Unless explicitly stated, the parameter configuration shown in Table 2 is used. The slot length is set to $\Delta = \min(\tau_1, \tau_2)$.

After examining various numerical examples of our stability analysis in Sect. 4, we found that the control parameter γ is hardly affected stability of the XCP protocol. In this paper, we therefore focus only on the effect of con-

trol parameters α and β[†].

Also, we found that the output link bandwidth C of an XCP router did not affect stability of the XCP protocol. Although the proof is not shown in this paper due to space limitation, independence of the output link bandwidth C from stability of the XCP protocol can be confirmed from the fact that expansion of Eq. (19) eliminates all C's. This phenomenal finding will be confirmed through simulation experiments in Sect. 5.2.

5.2 Effect of Propagation Delays

First, the effect of propagation delays of XCP flows on stability of the XCP protocol is investigated. Figure 3 shows stability regions of XCP control parameters (α β) for different settings of two-way propagation delays: i.e., $(\tau_1, \tau_2) = (10, 10), (20, 20), (10, 20)$, and $(10, 30)$ [ms]. The stability region is a region surrounded by the boundary line in the figure, and the vertical and the horizontal axes. XCP operates stably only when XCP control parameters (α, β) lie in the stability region. Note that in Fig. 3, boundary lines for (τ_1, τ_2) = (10, 10) and (20, 20) are almost identical.

In the following simulations, all XCP flows are activated simultaneously at $t = 0$. Note that staggered activation of XCP flows, instead of simultaneous activation, does not affect the stability of the XCP protocol if the activation interval of consecutive XCP flows is larger than the average round-trip time.

Figure 3 indicates that the stability region in a heterogeneous case (i.e., when two-way propagation delays τ_1 and τ_2 are different) is larger than that in the homogeneous case (i.e., when two-way propagation delays τ_1 and τ_2 are identical). This phenomenon can be explained by de-synchronization of XCP flows with different propagation delays; i.e., when XCP flows have different propagation delays, variation in the transfer rate of an XCP flow is likely to be canceled by those of other XCP flows. Moreover, Fig. 3 indicates that in homogeneous cases (i.e., when two-way
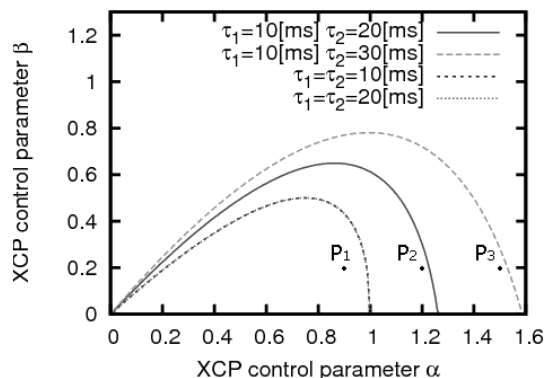
Table 2 The parameter configuration use in numerical examples and simulation results.

C	400 [Mbit/s]
τ_1	10 [ms]
τ_2	20 [ms]
N_1	10
N_2	10
γ	0.1

Fig. 3 Stability region of XCP control parameters (α β) for different settings of two-way propagation delays (τ_1, τ_2); the stability region in a heterogeneous case is larger than that in the homogeneous case.

[†]Note that it is shown in [15] that the control parameter γ does affect efficiency of the XCP router and fairness among XCP flows.

propagation delays of all XCP flows are identical) the stability region is independent of two-way propagation delays τ_1 and τ_2.

From these observations, we conclude that when XCP flows are heterogeneous, XCP operates more stably than the case when XCP flows are homogeneous.

We then examine the accuracy of our approximate analysis. We choose three settings of control parameters (α, β): $P_1 = (0.9, 0.2)$, $P_2 = (1.2, 0.2)$, and $P_3 = (1.5, 0.2)$ as shown in Fig. 3. For each control parameters setting, we perform simulation using ns-2 simulator for the same topology with Fig. 2. These control parameters settings are chosen to examine validity of our approximate analysis. For instance, if our stability analysis is valid, simulation results with P_2 should be stable for $(\tau_1, \tau_2) = (10, 20)$, $(10, 30)$ and unstable for $(\tau_1, \tau_2) = (10, 10)$, $(20, 20)$. In all simulations, the packet size is 1,000 [byte] and the initial window size is 1 [packet]. In all simulations, all XCP flows are activated at 0 [s], the initial window size is set to 1 [packet], and the network topology shown in Fig. 2 is used.

Simulation results for control parameters settings P_1, P_2, and P_3 are shown in Figs. 4 through 6, respectively. These figures show evolution of the window size of an XCP flow in flow class 1 for different settings of two-way propagation delays: i.e., $(\tau_1, \tau_2) = (10, 10)$, $(20, 20)$, $(10, 20)$, and $(10, 30)$. For each simulation result, stability of XCP is determined using a simple criterion — whether the window size of an XCP flow at the end of simulation is within ± 5% of its average value.

These simulation results are in agreement with our analytic results. For instance, the stability region shown in Fig. 3 indicates that, with the control parameters of $P_2 = (1.2, 0.2)$, the operation of XCP flows is unstable for $(\tau_1, \tau_2) = (10, 10)$ and $(20, 20)$, and is stable for $(\tau_1, \tau_2) = (10, 20)$ and $(10, 30)$. Simulation results shown in Fig. 5 clearly show that the operation of XCP flows is unstable for $(\tau_1, \tau_2) = (10, 10)$ and $(20, 20)$. Similar tendency can be observed for other control parameters $P_1 = (0.9, 0.2)$ and $P_3 = (1.5, 0.2)$. From these observations, we confirm validity of our approximate analysis.

Figures 4 through 6 include simulation results for $(\tau_1, \tau_2) = (10, 20)$ with a large output link bandwidth $C = 800$ [Mbit/s]. One can find from these figures that stability of the XCP protocol is not affected by the output link bandwidth. As we have discussed in Sect. 5.1, these results coincide with our finding; i.e., the independence of the output link bandwidth C from stability of the XCP protocol.

5.3 Effect of Variation in Propagation Delays

Next, the effect of variation in propagation delays of XCP flows on stability of the XCP protocol is investigated. In this paper, CV (Coefficient of Variation) is used to measure variation in propagation delays, which is defined by

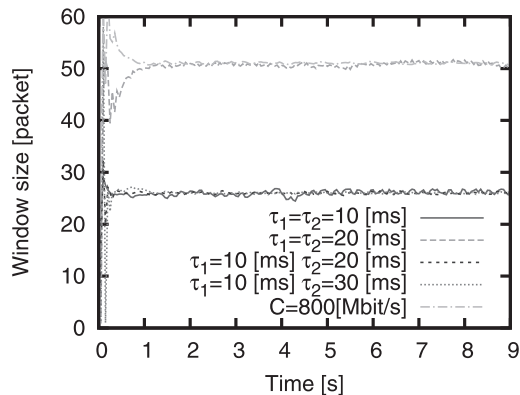$$CV = \frac{1}{d} \sqrt{\frac{\sum_{i=1}^{M}(\tau_i - d)^2}{\sum_{i=1}^{M} N_i}}. \tag{22}$$

Fig. 4 Simulation results with the control parameters of $P_1 = (0.9, 0.2)$; the window size of an XCP flow in flow class 1 is stable regardless of the two-way propagation delays (τ_1, τ_2).
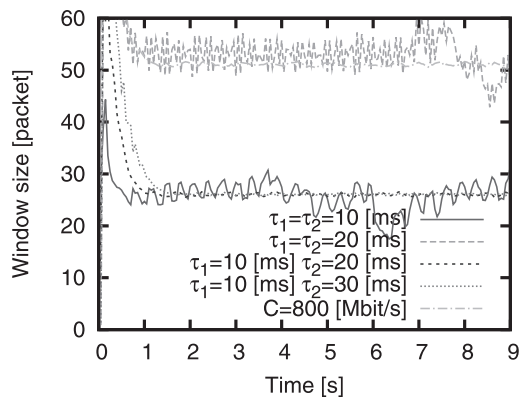

Fig. 5 Simulation results with the control parameters of $P_2 = (1.2, 0.2)$; the window size of an XCP flow in flow class 1 is unstable for $(\tau_1, \tau_2) = (10, 10)$, $(20, 20)$.
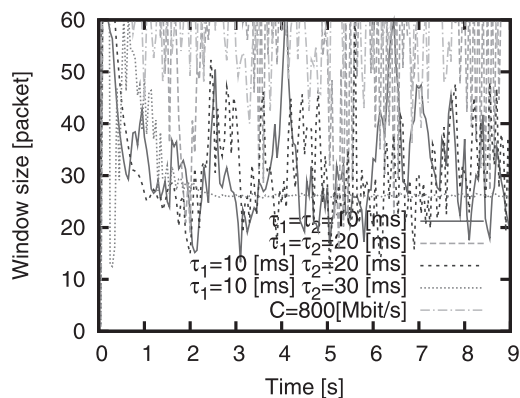

Fig. 6 Simulation results with the control parameters of $P_3 = (1.5, 0.2)$; the window size of an XCP flow in flow class 1 is stable only when the two-way propagation delays (τ_1, τ_2) are set to $(10, 30)$.

Figure 7 shows stability regions of XCP control parameters (α, β) for different numbers of XCP flows in each flow class: i.e., $(N_1, N_2) = (5, 15)$, $(10, 10)$, and $(15, 5)$. In this figure, propagation delays of XCP flows, τ_1 and τ_2, are set to 10 [ms] and 20 [ms], respectively.
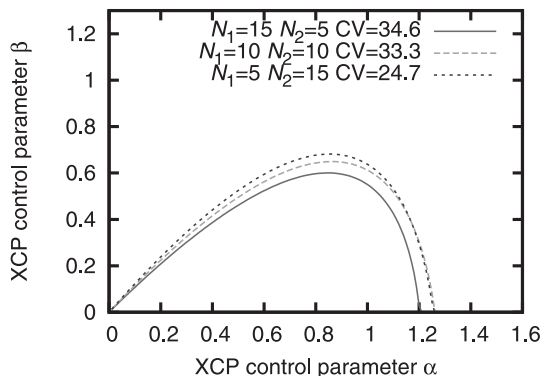
Fig. 7 Stability region of XCP control parameters (α β) for different numbers of XCP flows in each flow class (N_1, N_2); the stability region is smallest when (N_1, N_2) = (15, 5).

Fig. 8 Maximum modulus of eigenvalues of the state transition matrix **B** for $\tau_1 = 10$ [ms], $N_2 = 1$, and (α,β) = (0.4,0.226); the operation of XCP becomes unstable when the number of XCP flows in flow class 1, N_1, reaches around 100 for $\tau_2 = 200$ [ms].

Fig. 9 Evolution of the window size of an XCP flow in flow class 1 for $\tau_1 = 10$ [ms] and (α, β) = (0.4, 0.226); XCP flows in flow class 1 are stable regardless of the two-way propagation delay τ_2 of flow class 2. Maximum throughput are 4.00 [Mbit/s] for $\tau_2 = 100$ [ms] and 200 [ms].

Fig. 10 Evolution of the window size of an XCP flow in flow class 2 for $\tau_1 = 10$ [ms] and (α, β) = (0.4, 0.226); XCP flows in flow class 2 become unstable when the two-way propagation delay τ_2 of flow class 2 is large. Maximum throughput are 4.00 [Mbit/s] for $\tau_2 = 100$ [ms] and 200 [ms].

Figure 7 shows that the stability region is smallest when (N_1, N_2) = (15, 5); i.e., when the number of XCP flows in flow class 1 is larger than that in flow class 2. This phenomenon can be explained as follows. As explained in Sect. 2, both the efficiency controller and the fairness controller are invoked every average round-trip time of XCP flows. When there exist many XCP flows with a small propagation delay, the average round-trip time estimated by the XCP router tends to be small. Since the XCP router invokes its controllers every the average round-trip time, these controllers are invoked quite frequently. This results in aggressive control of the XCP router, leading unstable operation.

From these observations, we conclude that when variation in propagation delays of XCP flows is large, operation of XCP becomes unstable.

We then investigate the effect of heterogeneity in XCP flows on stability of the XCP protocol. Figure 8 shows the maximum modulus of eigenvalues of the state transition matrix **B** for different numbers of XCP flows in flow class 1, N_1. In this figure, the number of XCP flows in flow class 2, N_2, is fixed at 1, and the propagation delay of XCP flows in flow class 1, τ_1, is at 10 [ms]. Note that control parameters (α, β) are set to their recommended values, (0.4, 0.226) [6].

Figure 8 shows, for example, the operation of XCP becomes unstable when the number of XCP flows in flow class 1, N_1, reaches around 100 (i.e., the maximum modulus becomes larger than 1.0) for $\tau_2 = 200$ [ms].

Finally, through simulation experiments, we confirm the validity of our stability analysis and also investigate how XCP operates unstably when the heterogeneity of XCP flows is too large.

Figures 9 through 11 show evolution of the window size of an XCP flow in each flow class, and the evolution of the queue length of the XCP router. In these figures, the number of XCP flows in each flow class, (N_1, N_2), are set to (99, 1). Also, the two-way propagation delay of each flow class, (τ_1, τ_2), are to either (10, 100) or (10, 200). Figure 9 is the simulation result of XCP flows with a small propagation delay. Figure 10 is the simulation result of XCP flows with a long propagation delay.
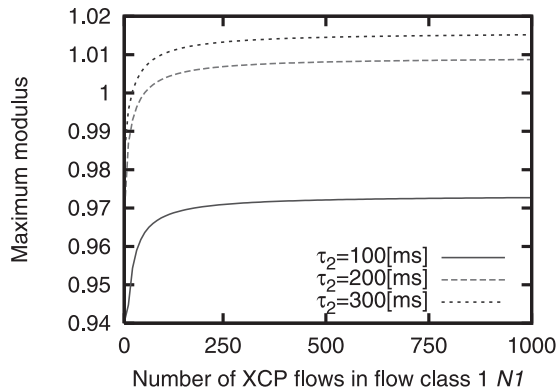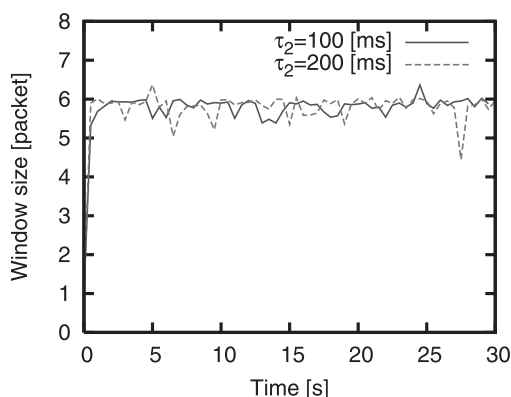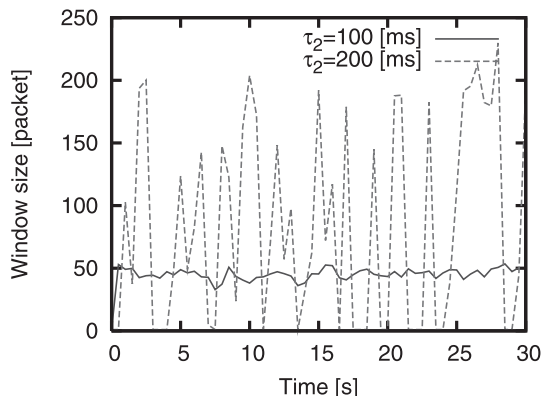
Figures 10 and 11 indicate that, when the two-way propagation delay τ_2 of the XCP flow in flow class 2 is 200 [ms], its window size and the queue length of the XCP
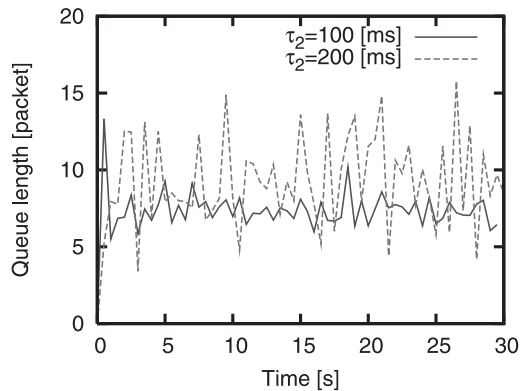
Fig. 11 Evolution of the queue length of the XCP router for $\tau_1 = 10$ [ms] and $(\alpha, \beta) = (0.4, 0.226)$; The XCP router becomes unstable when the two-way propagation delay τ_2 of flow class 2 is large.

router show oscillatory behavior, leading low throughput. Namely, when the variation in propagation delays of XCP flows is large, the window size of the XCP flow and the queue length of the XCP router become unstable, which shows the validly of our stability analysis.

6. Conclusion

In this paper, we have analyzed the stability of XCP in a network with heterogeneous XCP flows (i.e., XCP flows with different propagation delays). Through several numerical examples and simulation results, we have investigated the effect of system parameters and XCP control parameters on stability of the XCP protocol. Our findings include: (1) when XCP flows are heterogeneous, XCP operates more stably than the case when XCP flows are homogeneous, (2) conversely, when variation in propagation delays of XCP flows is large, operation of XCP becomes unstable, and (3) the output link bandwidth of an XCP router is independent of stability of the XCP protocol.

As future work, we are planning to analyze the transient performance of XCP utilizing our fluid model of XCP. In addition, we are planning to derive the optimal configuration of XCP control parameters, which maximizes the performance of XCP, based on our stability analysis and transient performance analysis. We are planning to clarify the stability of XCP in a network with frequent XCP flows.

Acknowledgements

References

[1] J. Postel, "Transmission control protocol," Request for Comments (RFC) 793, Sept. 1981.

[2] J. Padhye and S. Floyd, "On inferring TCP behavior," ACM SIG-COMM Computer Communication Review, vol.31, no.4, pp.287– 298, Aug. 2001.

[3] S. Floyd, "Highspeed TCP for large congestion windows," Request for Comments (RFC) 3649, Dec. 2003.

[4] H. Bullot, R.L. Cottrell, and R. Hughes-Jones, "Evaluation of advanced TCP stacks on fast long-distance production networks," Proc. PFLDnet 2004, Feb. 2004.

[5] R. Wang, G. Pau, K. Yamada, M.Y. Sanadidi, and M. Geria, "TCP startup performance in large bandwidth delay networks," Proc. IEEE INFOCOM 2004, pp.796–805, March 2004.

[6] D. Katabi, M. Handley, and C. Rohrs, "Congestion control for high bandwidth-delay product networks," Proc. ACM SIGCOMM 2002, pp.89–102, Aug. 2002.

[7] K. Ramakrishnan, S. Floyd, and D.B. Rosen, "The addition of explicit congestion notification (ECN) to IP," Request for Comments (RFC) 3168, Sept. 2001.

[8] M. Welzl, "Scalable router aided congestion avoidance for bulk data transfer in high speed networks," Proc. PFLDnet2005, Feb. 2005.

[9] Y. Xia, L. Subramanian, I. Stoica, and S. Kalyanaraman, "One more bit is enough," Proc. ACM SIGCOMM 2005, pp.37–48, Aug. 2005.

[10] A. Falk and D. Katabi, "Specificaton for the explicit control protocol(XCP)," IETF Internet Draft: draft-falk-xcp-spec-01.txt, Oct. 2005.

[11] D. Katabi, "XCP's performance in the presence of malicious flows," Proc. PFLDnet 2004, Feb. 2004.

[12] Y. Zhang, D. Leonard, and D. Loguinov, "Jetmax: Scalable max-min congestion control for high-speed heterogeneous networks," Proc. IEEE INFOCOM 2006, pp.1–13, April 2006.

[13] Y. Zhang and M. Ahmed, "A control theoretic analysis of XCP," Proc. IEEE INFOCOM 2005, pp.2831–2835, March 2005.

[14] H. Balakrishnan, N. Dukkipati, N. McKeown, and C. Tomlin, "Stability analysis of explicit congestion control protocols," IEEE Commun. Lett., vol.11, no.10, pp.823–825, Oct. 2007.

[15] S.H. Low, L.L.H. Andrew, and B.P. Wydrowski, "Understanding XCP: Equilibrium and fairness," Proc. IEEE INFOCOM 2005, pp.1025–1036, March 2005.

[16] H. Hisamatsu, H. Ohsaki, and M. Murata, "Fluid-based analysis of network with DCCP connections and RED routers," Proc. IEEE SAINT 2006, pp.156–163, Jan. 2006.

[17] N.S. Nise, Control Systems Engineering, 4th ed., John Wiley & Sons, New York, 2003.

Yusuke Sakumoto received B.E. and M.E. degrees in the Information and Computer Sciences from Osaka University in 2006 and 2008, respectively. He is currently a Ph.D. candidate Department of Information Networking, Graduate School of Information Science and Technology, Osaka University, Japan. His research work is in the area of congestion control protocol. He is a student member of IEEE and IPSJ.

Hiroyuki Ohsaki   received the M.E. degree in the Information and Computer Sciences from Osaka University, Osaka, Japan, in 1995. He also received the Ph.D. degree from Osaka University, Osaka, Japan, in 1997. He is currently an associate professor at Department of Information Networking, Graduate School of Information Science and Technology, Osaka University, Japan. His research work is in the area of traffic management in high-speed networks. He is a member of IEEE.

Makoto Imase   received his B.E. and M.E. degrees in information engineering from Osaka University in 1975 and 1977, respectively. He received D.E. degree from Osaka University in 1986. From 1977 to 2001, he was engaged Nippon Telegraph and Telephone Corporation (NTT). He has been a Professor of Graduate School of Information Science and Technology at Osaka University since 2002. His research interests are in the area of information networks, distributed systems and graph theory. He is a member of IPSJ and JSIAM.